Simulation of the Effects of Bathymetry and Land–Sea Contrasts on Hurricane Development Using a Coupled Ocean–Atmosphere Model

N. CUBUKCU

Department of Meteorology, The Florida State University, Tallahassee, Florida

R. L. PFEFFER

Geophysical Fluid Dynamics Institute and Department of Meteorology, The Florida State University, Tallahassee, Florida

D. E. DIETRICH

Center for Air–Sea Technology, Mississippi State University, Mississippi State, Mississippi

(Manuscript received 17 September 1998, in final form 10 May 1999)

ABSTRACT

A version of the Naval Research Laboratory Limited Area Dynamical Weather Prediction Model is coupled with the DieCAST ocean circulation model, which is particularly well suited for the specification of realistic bathymetry. The resulting coupled model, with 11 levels in the atmosphere and 20 in the ocean, is used to study the sensitivity of hurricane formation, intensification, and weakening in the Gulf of Mexico and the Carribean region to the presence of land–sea contrasts and bathymetry in this region. Numerical simulations with the fully coupled model, Gulf of Mexico, and Carribean geography and bathymetry are compared with simulations with coupling and no geometry or bathymetry and also with simulations using the uncoupled atmospheric model.

The primary finding is that land–sea contrast and bathymetry reduce the intensification of the tropical disturbance, even when the hurricane is far from shore. The effect of drier air coming off the land masses surrounding the Gulf, which can penetrate to the storm center in a day, is to reduce the moisture supply and thereby decrease the rate of intensification of the storm. This is true in both the coupled and uncoupled model integrations. In the coupled model simulations, inertia currents and vertical mixing and upwelling on the continental shelf cause more intense and more widespread sea surface cooling in the presence of land–sea contrasts and bathymetry than in its absence, further reducing the rate of intensification.

1. Introduction

The effect of sea surface temperature (SST) on the genesis and intensification of tropical cyclones is well known. It has long been recognized that a necessary condition for the development of tropical disturbances into hurricanes is that the SST exceed 26°C. Observational studies (e.g., Leipper 1967) and numerical studies (e.g., O'Brien and Reid 1967) have also established that tropical cyclones have a marked feedback effect on the ocean, lowering the SST as a result of upwelling and mixing associated with low pressure and strong surface winds.

Numerous studies in the past have dealt with either the response of the ocean to a tropical cyclone using an ocean model with specified atmospheric forcing (e.g., Chang and Anthes 1978; Price 1981; Cooper and Thompson 1989; Ginis and Dikinov 1989), or the genesis of a hurricane using an atmospheric model with specified SST (e.g., Sundqvist 1970; Kurihara and Tuleya 1974; Rosenthal 1978; Chang and Madala 1980; Pfeffer and Challa 1981, 1992; Challa and Pfeffer 1990). Studies by Tuleya et al. (1984) and Tuleya (1994) of the effect of landfall on cyclone intensity were also based on the use of an atmospheric model with the SST specified.

The earliest investigations using a coupled atmosphere–ocean model to simulate the interaction between a tropical cyclone and the ocean were made by Chang and Anthes (1979) and Sutyrin and Khain (1979). The essential findings of these studies were that sea surface cooling due to storm-induced turbulent mixing and upwelling reduces the latent and sensible heat transfer from the ocean to the atmosphere, with a resulting decrease in the intensity of the atmospheric disturbance. Sutyrin

Corresponding author address: Dr. Nihat Cubukcu, Department of Meteorology, 411 Love Building, The Florida State University, Tallahassee, FL 32306.
E-mail: nihat@io.met.fsu.edu

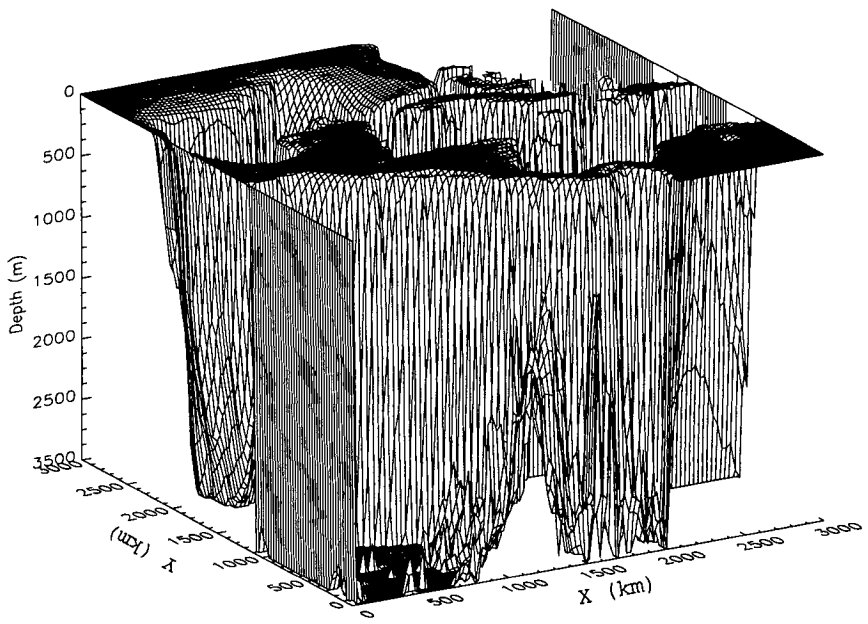

FIG. 1. The topography of the model domain (used for experiments A2 and C2).

and Khain (1984) found, however, that this cooling effect is reduced when the oceanic mixed layer is deeper, and that the feedback of the cooling on the atmospheric disturbance is of less consequence when the disturbance travels faster. These findings have been confirmed by Khain and Ginis (1991), who also studied the effect of the ocean–air interaction on the path of the hurricane. More recently, Bender et al. (1993) found that the ocean response was quicker by about 12 h when they employed a numerical model with higher resolution than the ones used in the earlier studies.

Among the aforementioned studies, the only ones dealing with the effect of bottom topography or land–sea contrasts were those by Cooper and Thompson, Tuleya et al., and Tuleya. Cooper and Thompson (1989), using an ocean model with no coupling to an atmospheric model, found that bottom topography in the Gulf of Mexico causes strong inertial currents and produces a storm surge along the coast. Tuleya et al. (1984) and Tuleya (1994), using an atmospheric model with no coupling to an ocean model, showed how radiation processes over land act to damp the intensity of a hurricane as it makes landfall, even over wet land. None of the *coupled* model studies to date, however, take into account continental and bathymetrical influences. It is the purpose of the present study to investigate the effects of land–sea contrast and bathymetry in a fully coupled atmosphere–ocean model.

The inclusion of bathymetry requires the use of an ocean model with very fine resolution in the vertical in order to resolve the surface and boundary layers. Most ocean models that have been employed in the past are not capable of resolving shallow shelf topography and the associated boundary layers. Moreover, previous studies with coupled models have focused only on the interactions between a mature hurricane and the ocean. In such studies, the sudden imposition of strong atmospheric forcing on an ocean at rest causes unrealistically large inertial oscillations. The duration of these oscillations is comparable to that of the atmospheric forcing, thereby complicating the study of the ocean–air interactions. In the present study we use a high-resolution atmosphere–ocean model to investigate the complete life cycle of a tropical disturbance as it intensifies from a weak depression in the Carribean and travels through the Gulf of Mexico. The model consists of the Naval Research Laboratory Limited Area Dynamical Weather Prediction Model (Madala et al. 1987) coupled to the Dietrich Center for Air–Sea Technology (DieCAST) general ocean circulation model (Dietrich and Ko 1994). The model domain encompasses the Gulf of Mexico, the Carribean, and the western Atlantic from 5° to 34°N and from 97° to 68°W, an area of about 3220 km on a side. The maximum observed ocean depth in this region is about 6 km. In the ocean model, we chose a maximum depth of 3.5 km, because atmospheric forcing hardly impacts the deep ocean (J. J. O'Brien 1996, personal communication). Figure 1 is a three-dimensional depiction of this domain.

In this paper we compare the results of simulations of tropical cyclone development using an uncoupled atmospheric model with and without land–sea contrast and a coupled atmosphere–ocean model with and without bathymetry and land–sea contrast. The initial conditions for all model simulations consist of a uniform SST and an ocean at rest, with atmospheric winds and pressures specified from McBride and Zehr's (1981) composite Atlantic prehurricane depression (determined

from tropical disturbances mostly in the domain we have chosen for our study).

The ocean model is described in section 2 and the atmosphere model in section 3. The method of coupling is discussed in section 4 and the results of various simulations with the coupled model are reported in section 5. Our conclusions and suggestions for future research are presented in section 6.

2. Ocean model

a. Model description

The ocean model adopted for this study is one that has been used extensively in climatological applications to simulate ocean and lake circulations (see, e.g., Dietrich and Roache 1991; Dietrich and Lin 1994; Dietrich and Ko 1994). Previous applications of this model to the Gulf of Mexico have led to a better understanding of the ocean dynamics in this region (Dietrich and Roache 1991; Dietrich and Lin 1994). The ocean model equations can be found in Dietrich and Ko (1994). No-slip boundary conditions along the rigid boundaries are used. For our application, we consider an ocean basin as a closed system with no inflow or outflow across its boundaries. At the surface, a rigid-lid approximation is used, which allows heat and momentum exchange with the atmosphere but does not allow high-frequency variations of the surface height such as those associated with surface gravity waves. It does, however, allow displacements on timescales over which storm surges occur. To parameterize momentum and heat exchange processes, the model uses the bulk formulas

$$\tau^x = \rho_{\text{atm}} C_D U(u_{\text{atm}} - u_{\text{sea}}) \tag{1}$$

$$\tau^y = \rho_{\text{atm}} C_D U(v_{\text{atm}} - v_{\text{sea}}) \tag{2}$$

$$F_S = \rho_{\text{atm}} C_P C_H U(T_{\text{atm}} - T_{\text{sea}}) \tag{3}$$

$$F_Q = \rho_{\text{atm}} L C_H U(q_{\text{atm}} - q_{\text{sea}}), \tag{4}$$

where

$$U = \sqrt{(u_{\text{atm}} - u_{\text{sea}})^2 + (v_{\text{atm}} - v_{\text{sea}})^2}, \tag{5}$$

τ^x and τ^y denote momentum fluxes in eastward and northward directions, and F_S and F_Q denote sensible and latent heat fluxes, respectively. Here C_D and C_H are drag coefficients for momentum and heat; and C_P and L are the specific heat capacity of the air at constant pressure, and the latent heat coefficient, respectively. The subscript "atm" denotes values at 10-m height above the sea surface, and the subscript "sea" denotes the values at the sea surface. Here C_D is a function of the wind speed at 10 m, whereas C_H is assumed to be a constant. By relating C_D to the wind speed, the model implicitly takes into account the effects of the surface roughness. DieCAST includes vertical and horizontal diffusion within the ocean, which are approximated by mixing-length theory. The horizontal diffusion coefficient has the value of 100 $m^2\ s^{-1}$. The vertical eddy diffusion coefficients for momentum and heat, which depend on the degree of turbulence in the flow rather than on the physical properties of the fluid, are defined in terms of the Richardson number as follows:

$$K_H = \text{DMZ0} + 2.5\frac{\tau}{(1 + 10\text{Ri})^{1.5}} \tag{6}$$

$$K_M = \text{DMZ0} + 5\frac{\tau}{(1 + 10\text{Ri})^{1.5}}. \tag{7}$$

Here, $\tau = \sqrt{\tau_x^2 + \tau_y^2}$, DMZ0 is a constant (10 $cm^2\ s^{-1}$), and Ri is Richardson number

$$\text{Ri} = \frac{\dfrac{g}{\rho_0}\dfrac{\partial \rho}{\partial z}}{\left(\dfrac{\partial u}{\partial z}\right)^2}. \tag{8}$$

According to (6) and (7), the most rapid turbulent mixing due to wind stress occurs when Ri = 0 [i.e., when the buoyancy damping of turbulent kinetic energy (TKE) production is negligibly small]. The range of K_M and K_H throughout the time integration in the present model is between 10 and 30 $cm^2\ s^{-1}$. Most ocean models use a similar parameterization for vertical diffusion (see, e.g., Chang 1985) but require unrealistically large diffusion coefficients in order to control the energy cascade and keep the model computationally stable. As discussed by Dietrich and Roache (1991) smaller diffusion coefficients can be used in the DieCAST model because it is quite stable with more realistic coefficients. Dietrich and Lin (1994) have performed various experiments with different diffusion coefficients in the Gulf of Mexico and have found that smaller diffusion coefficients give temperature fields and currents that compare better with observations than those obtained with larger coefficients.

b. Numerical representation

In order to model the thin ocean surface boundary layer, a vertically stretched (log linear) coordinate is used. The stretched vertical coordinate S is defined (Dietrich et al. 1987) as

$$S(z) = C_1 z + C_2 L(z), \tag{9}$$

where

$$L(z) = \ln(z/z_0) \tag{10}$$

and z_0 is the surface roughness parameter. Here C_1 and C_2 can be found by setting $S(H) = H$, where H is the depth of the ocean, and $S(h) = nH/N = h$, where h is the expected mixed layer depth. Here n is the number of levels in the mixed layer and N is the number of levels in the model. Derivatives with respect to z can be found by

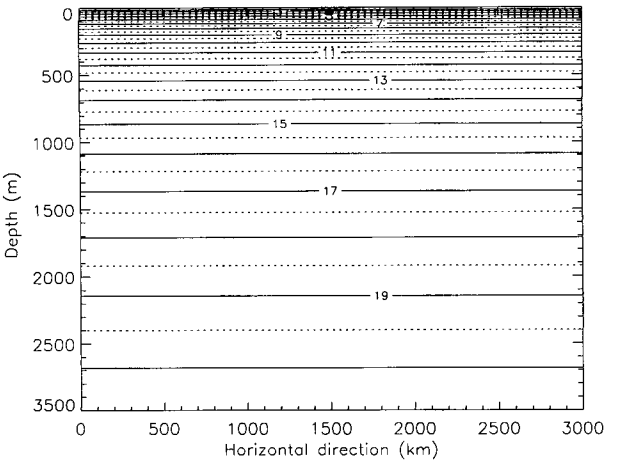

FIG. 2. Vertical cross section of the ocean model domain. The solid and dashed lines show the vertical velocity and pressure levels, respectively. The level numbers are shown on solid lines.

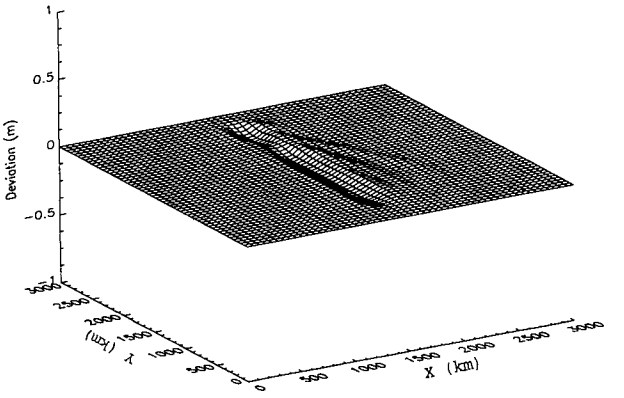

FIG. 3. Deviations in the free surface height with a nonstationary forcing, at day = 4.5. The forcing moves from south to the north in the middle of the model domain.

$$\frac{d(\ )}{dz} = \frac{ds}{dz}\frac{d(\ )}{ds}, \tag{11}$$

where

$$\frac{ds}{dz} = (C_1 + C_2/z). \tag{12}$$

The discretization of the equations is based on a control volume approach with semicollocated grids in which all terms in governing equations, except the pressure gradient term, are calculated at mass points of control volume boxes that fill the entire domain (Arakawa A-grid). At the boundaries, the boxes are considered to be either fully inside or outside the water. The pressure gradient term and the terms in the mass continuity equation are calculated at the lateral boundaries of each control volume (Arakawa C-grid). The advantage of this approach is that the A-grid gives more accurate representation of the Coriolis term and the C-grid a more accurate representation of the pressure gradient term (Dietrich 1993). The transformation between these grid points is performed by linear interpolation. The boundaries are artificially approximated by stair-step segments. The horizontal resolution is uniform with $\Delta x = \Delta y = 30$ km. As seen in Fig. 2, there are 20 layers from the surface to the ocean floor with the thicknesses of 10.6, 13.2, 16.4, 20.6, 25.6, 31.6, 40, 50, 62, 77, 96, 120, 150, 186, 231, 290, 360, 460, 560, and 700 m, respectively.

The time integration scheme, which we call the "filtered leapfrog trapezoidal weighted" (FLTW) scheme, is a weighted combination of the leapfrog and filtered leapfrog trapezoidal (FLT) scheme (Roache and Dietrich 1988). The FLT scheme has been analyzed for one-dimensional, constant coefficient, advection equation and has been shown to have advantages for quasi-steady flows (Dietrich et al. 1987). The FLTW scheme retains that accuracy. The purpose of using this method is to prevent the time-splitting instability that occurs when the conventional leapfrog method is used. The Courant number of the FLTW scheme has been analyzed by Roache and Dietrich (1988), who found a stability limit of

$$C \leq 1 - \frac{w}{2}, \tag{13}$$

where w is a weight to be assigned. For $w = 0$, the stability limit reduces to the conventional restriction of $C \leq 1$. For $w = 1$ (the value we use), the stability limit is $C \leq 0.5$. This value has been verified experimentally by Roache and Dietrich (1988).

c. *Test of the model*

The ocean model was tested in an idealized square basin 3000 km on a side without coupling to the atmosphere model (Cubukcu 1997). In these tests, the distribution and magnitude of the sea surface cooling and the inertia waves that developed in response to idealized stationary and moving axisymmetrical hurricane vortices of constant intensity were found to be similar to those reported by previous investigators (Chang and Anthes 1978, 1979; Cooper and Thompson 1989; Bender et al. 1993). For example, when the surface velocity fields were compared with those of Chang and Anthes (1978), it was found that the rightward bias and scale of the region affected by the tropical storm are quite similar. The velocity fields were also compared with those in an observational study by Sanford et al. (1987) for Hurricanes Norbert and Josephine and were found to agree reasonably well with their observations. Moreover, an experiment with ocean bottom topography displayed a storm surge along the coast. The difference in sea surface height in model integrations with and without bathymetry is illustrated in Figs. 3 and 4.

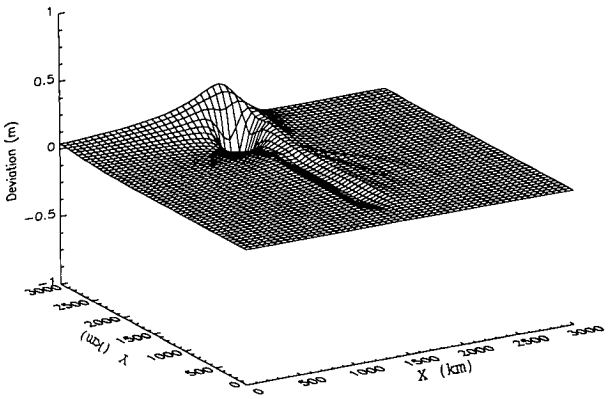

FIG. 4. Same as 3 except with bottom topography.

3. Atmospheric model

The atmospheric model employed in the present study is a version of the Naval Research Laboratory Limited Area Dynamical Weather Prediction Model (Madala et al. 1987) that has been used extensively to study the ingredients required for tropical disturbances to develop into hurricanes or typhoons (Challa and Pfeffer 1990; Pfeffer and Challa 1992; Challa et al. 1998). The model has been shown to be capable of simulating the development of tropical disturbances that intensify into hurricanes in nature and the nondevelopment of those that do not.

Not all terms have the same timescale in the governing equations. For computational efficiency, a split-implicit time integration scheme is used in the atmospheric model to calculate the fast gravity and slow Rossby modes separately. This method uses a time step Δt having n subintervals, $\Delta\tau$ (we use $n = 4$). The terms representing gravity wave propagation are integrated in the subintervals and those representing Rossby wave propagation are integrated with Δt. In this way, all terms are treated on their proper timescales, and the CFL condition is satisfied for each of the modes. We use $\Delta t = 60$ s, implying $\Delta\tau = 15$ s. At each time step Δt, the pressure gradient and the mass divergence terms are corrected by adding the contributions from the calculations in the subintervals. The integration of the other terms is accomplished by transforming them from the grid scale to eigenfunction space using expansions of the dependent variables in terms of the natural gravity modes of the system, which is equal to the number of layers in the numerical model.

The lateral boundary conditions for the atmospheric model are sponge-layer conditions at the northern and southern boundaries, which do not allow reflection of waves from these boundaries, and cyclic continuity in the east–west direction. No net mass fluxes are allowed on the northern and southern boundaries of the domain. The horizontal resolution is assumed to be uniform with $\Delta x = \Delta y = 30$ km.

The vertical coordinate σ is defined as the ratio of the local pressure to the surface pressure. The atmosphere is divided into 11 layers. Velocity, temperature, specific humidity, and geopotential height fields are defined in the middle of each layer and the other variables are defined at the boundaries between the layers (see Fig. 5). The surface fluxes are parameterized by bulk aerodynamic formulas as described in the ocean model. Inasmuch as the surface ocean currents under hurricane conditions can be as large as 3 m s^{-1}, inclusion of the upper ocean current in the surface flux calculation has a nonnegligible effect on the air–sea interactions.

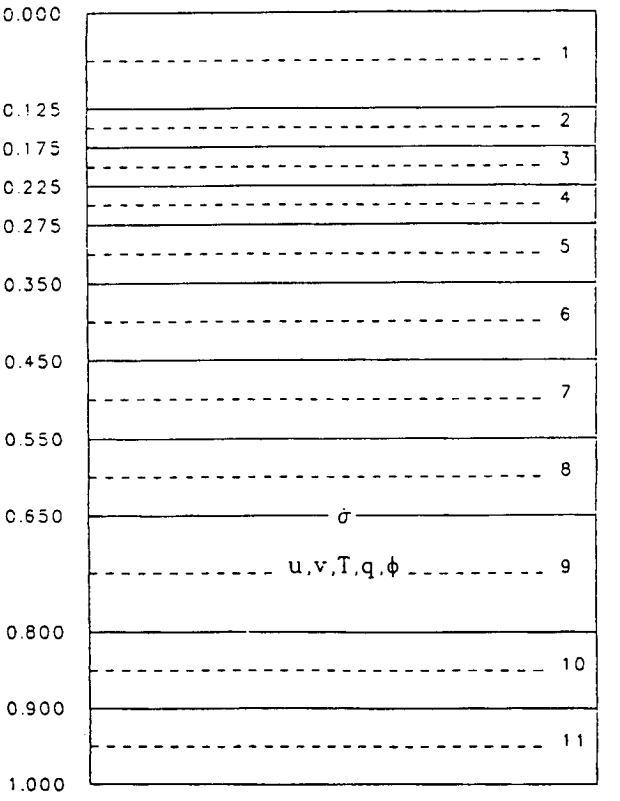

FIG. 5. Vertical cross section of the atmospheric model domain.

Over land, the surface fluxes are determined in nature by the heat balance and ground hydrology. To specify these properly, one would need detailed information that is not readily available in the composite dataset. Instead, we specified a fixed value for C_D that is much greater, and a fixed value for C_H that is much less, than the corresponding values over the sea. For the present purpose we also treat all land regions as flat surfaces.

Cumulus convection in the atmosphere is parameterized with the modified Kuo scheme. When there is no cumulus convection, and the relative humidity is greater than 96%, stable latent heating is turned on. Radiation is neglected in the model.

4. Coupling

Air–sea interactions affect both the ocean and the hurricane. Hurricanes transmit energy, momentum, and

vorticity to the water below, creating local oceanic perturbations, the intensities of which depend on the magnitude of the forcing. As the vortex moves away from a region, the perturbations left behind become weaker and eventually vanish. During this process, the upper layers of the ocean cool due to upwelling and turbulent mixing, as well as due to evaporation and sensible heat loss to the atmosphere. The rate of intensification of the tropical storm, in turn, depends on the SST. When the disturbance passes over land, the smaller heat and moisture flux from the surface and the larger frictional dissipation combine to weaken the vortex. If it subsequently travels over warm water, the disturbance can reintensify. In order to account properly for the various processes that influence tropical cyclone development, including air–sea interactions, it is necessary to employ a coupled atmosphere–ocean model with sufficiently high spatial–temporal resolution. For the purposes of the present study, we coupled the two models discussed earlier by specifying the vertical fluxes of momentum and sensible and latent heat at the air–sea interface as a function of the ocean surface current and the wind velocity, temperature, and humidity at 10 m above the surface. Over land, the drag coefficient and the bulk coefficient for heat fluxes were taken as 2.5×10^{-3} and 1×10^{-3}, respectively. Over the ocean, the drag coefficient is a function of wind speed, and the bulk coefficient for heat fluxes is 3×10^{-3}. Since the land surface is typically warmer than the air in summer, the surface heat flux in these experiments is upward over land.

The time steps for advancing the atmosphere and ocean models were 60 and 600 s, respectively. The coupling procedure, similar to that used by Chang and Anthes (1979) and Bender et al. (1993), was as follows:

1) integrate the atmosphere model for 10 consecutive time steps;
2) calculate the mean values of the surface fluxes (vertical momentum, sensible and latent heat) at the 10th time step;
3) call the ocean model with calculated mean values of the surface fluxes and integrate the ocean model for 1 time step;
4) return to the atmosphere model for the next time step with the new surface currents and SST; and
5) repeat this procedure until the whole integration period is over.

5. Numerical simulations

The four numerical simulations we compare in this paper are as follows:

1) uncoupled atmospheric model without land–sea contrasts (A1),
2) uncoupled atmospheric model with land–sea contrasts (A2),

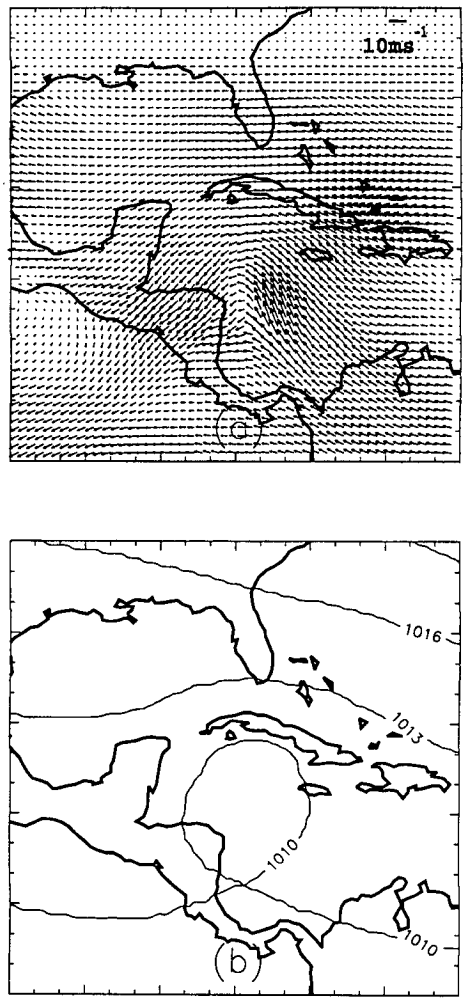

FIG. 6. Initial surface wind (a) and pressure (b) fields for the D2 dataset. Contour interval for surface pressure is 3 hPa.

3) coupled model without bathymetry and land–sea contrasts (C1),
4) coupled model with bathymetry and land–sea contrasts (C2)

Each simulation was carried out to 96 h.

The initial atmospheric pressure and wind fields for all model simulations were specified from McBride and Zehr's (1981) composite dataset for Atlantic prehurricane depressions D2 (determined from tropical disturbances mostly in the domain we have chosen for our study), as shown in Fig. 6. The dataset comprises the total meteorological fields, including disturbed and environmental fields. Pfeffer et al. (1990) analyzed the data for each elevation by conventional synoptic techniques and interpolated them to the grid locations for use in numerical models. The same data, which cover the Gulf of Mexico and some parts of the Atlantic Ocean, were used in several previous studies with the present atmospheric model (see, e.g., Challa and Pfeffer

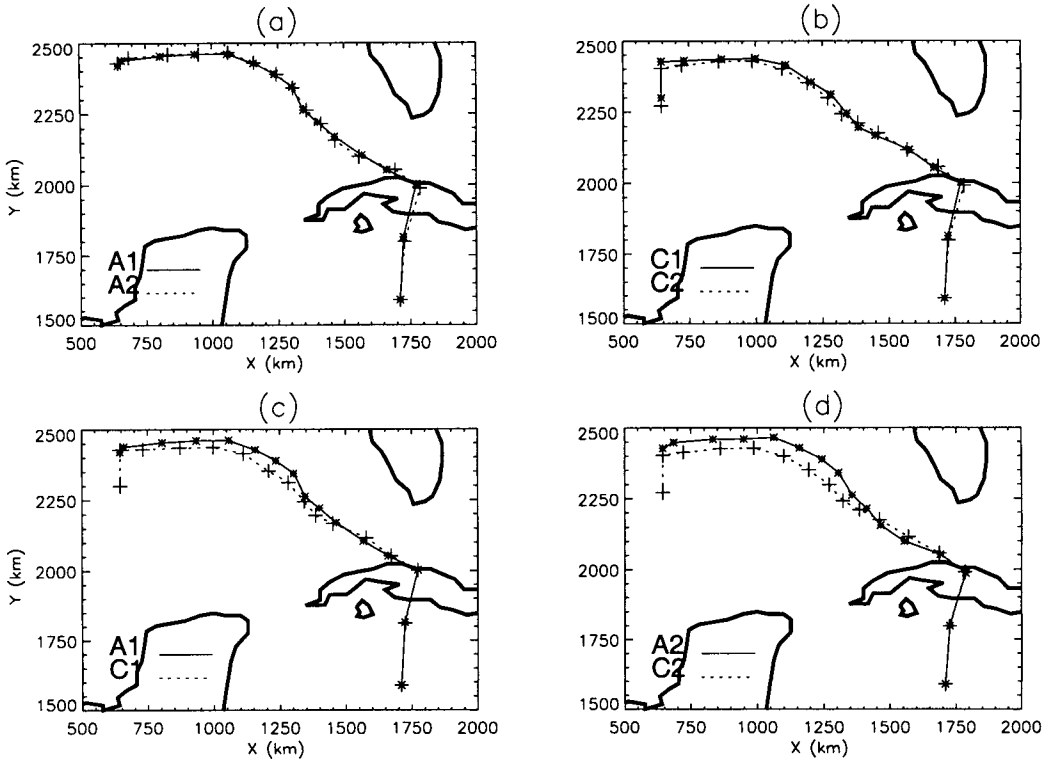

FIG. 7. Comparison of the storm track for first 90 h of time integration between (a) experiments A1 and A2; (b) C1 and C2; (c) A1 and C1; (d) A2 and C2. The first symbols from right represent the initial positions and others are plotted at every sixth hour.

1990) to investigate the mechanisms responsible for hurricane formation. In the present study, the center of the disturbance was placed initially at 19°N latitude and 81°W longitude.

The initial conditions for the ocean were taken to be an ocean at rest with a uniform sea surface temperature of 29.4°C, representing the mean August SST in the Gulf of Mexico (Bottomley et al. 1990), a mixed layer depth of 30 m, and a climatological mean vertical temperature profile within the ocean taken from Levitus (1982).

Experiments A1 and A2 were performed in order to isolate the effects of land–sea contrast when the disturbance is far from making landfall. Experiment A1 does not include land–sea contrast, whereas A2 includes it by specifying differences in surface drag and in the magnitudes of the heat and moisture coefficients. Orography on land is, however, omitted in this and the other experiments. The effect of land–sea contrast when the disturbance is far removed from land is a different problem from the one treated by Tuleya et al. (1984) and Tuleya (1994), in which the cloudiness associated with a disturbance making landfall is crucial to the radiation budget. We feel that the crude approximation we have used here to specify the difference between land and sea is justifiable within the context of the present study.

The coupled model experiment C1, without land–sea contrast and bathymetry, is very much like the experiments of Chang and Anthes (1979), Sutyrin and Khain (1979), Khain and Ginis (1991), Bender et al. (1993), and Mao (1994). Comparisons of the results of this experiment with those of experiment A1 are made to confirm consistency with the results of earlier studies and as a benchmark for comparison with experiment C2.

Experiment C2 is the first coupled model experiment of which we are aware that includes both bathymetry and land–sea contrast. Moreover, in both C1 and C2, the fine grid resolution of the ocean model in the horizontal and vertical directions provides a level of accuracy not generally achieved even in uncoupled model experiments. Such resolution is particularly important for resolving the bathymetry.

While our primary concern in this paper is the effect of land–sea contrast and bathymetry on the intensification and weakening of a hurricane, we mention briefly our results concerning the storm tracks, which are compared in Figs. 7a–d. These figures reveal very small differences in the tracks due to the presence or absence of land–sea differences and bathymetry (e.g., Figs. 7a,b) and a small, but significant, difference due to the mutual interactions of the ocean and atmosphere in the coupled models. In particular, the storms in the uncoupled models are displaced to the north of those in the coupled models (Figs. 7c,d). This is because the disturbances in

TABLE 1. The comparison of maximum surface wind speed and minimum surface pressure for the coupled and uncoupled experiments. A2 includes the land–sea contrasts and C2 includes the land–sea contrasts and bathymetry. A1 and C1 are without the land–sea contrasts and bathymetry.

Time (h)	V_{max} (m s^{-1}) A1–A2	P_s (hPa) A1–A2	V_{max} (m s^{-1}) C1–C2	P_s (hPa) C1–C2
12	17.7–18.5	1007–1006.9	16.4–17.0	1007.5–1007.4
24	25.6–22.8	999.7–1001.9	27.7–24.2	1001.2–1002.3
36	35.2–29.4	993.1–996.2	26.9–24.7	997.8–997.9
48	39.0–37.3	988.4–990.2	34.3–26.6	995.6–997.5
60	42.6–45.9	985.2–984.9	36.9–31.3	993.2–994.8
72	48.7–42.3	982.8–985.3	37.4–33.3	991.3–995.4
84	40.3–40.7	985.8–986.1	36.4–32.4	1001.7–1003.2
96	39.9–41.3	1008.8–1007.9	32.6–29.0	1009.2–1007.6

the coupled models are weaker than those in the uncoupled models and are thereby less affected by the β drift. This is consistent with results obtained by other investigators (see, e.g., Khain and Ginis 1991).

The differences in intensification among the different numerical experiments are shown in Table 1 and Figs. 8 and 9. Figures 8a and 9a and columns 2 and 3 of Table 1 reveal that the disturbance does not intensify as much in the presence of land–sea contrasts (A2) as it does when no land is present (A1), although the difference is small (3 m s^{-1} in maximum wind and 2 hPa in minimum surface pressure). During the weakening stage, after 84 h, the maximum wind speed and minimum surface pressure are nearly the same in the two experiments. Although the center of the disturbance remains far from land throughout most of the development stage, the effect of drier air coming off the landmasses surrounding the Gulf of Mexico (which can penetrate to the storm center in a day) is to reduce the moisture supply, and therefore the rate of intensification of the disturbance in A2 in comparison with that in A1. The role of clouds in the radiation budget of a disturbance undergoing landfall, which was treated by Tuleya (1994), is of less importance in the present problem.

Focusing next on Figs. 8c,d and 9c,d, we see that, consistent with the results of earlier studies, coupling significantly reduces the intensity of the hurricane. The average difference between A1 and C1 is 6 hPa in min-

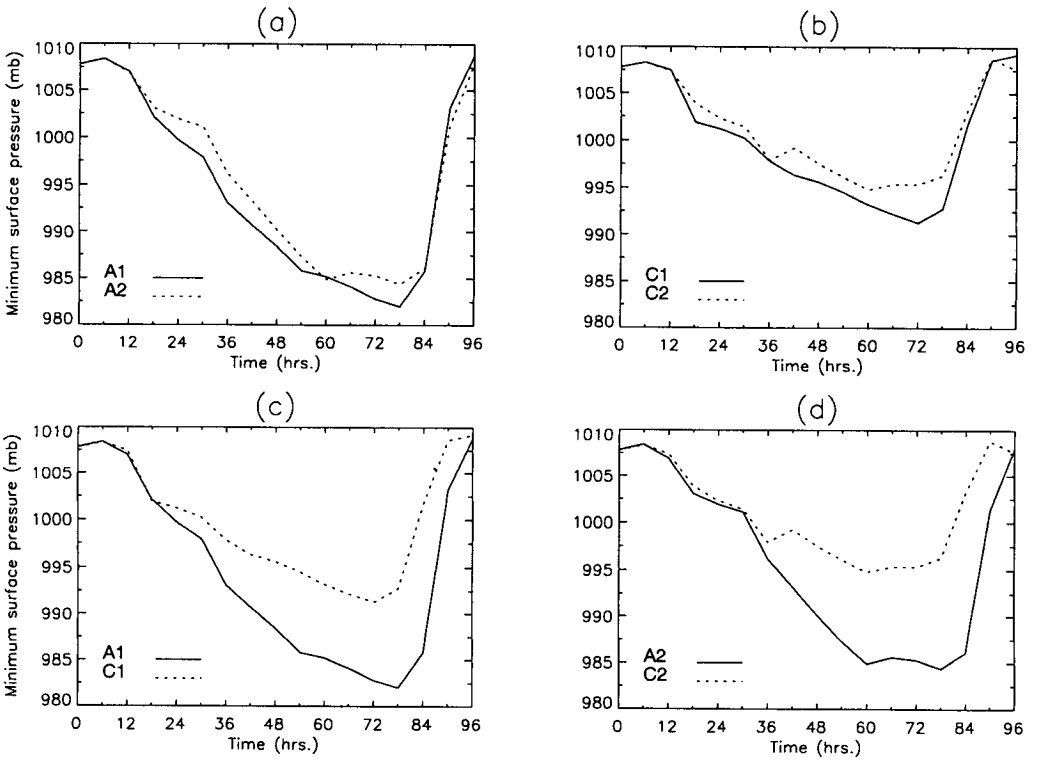

FIG. 8. Comparison of minimum surface pressure between (a) experiments A1 and A2; (b) C1 and C2; (c) A1 and C1; (d) A2 and C2.

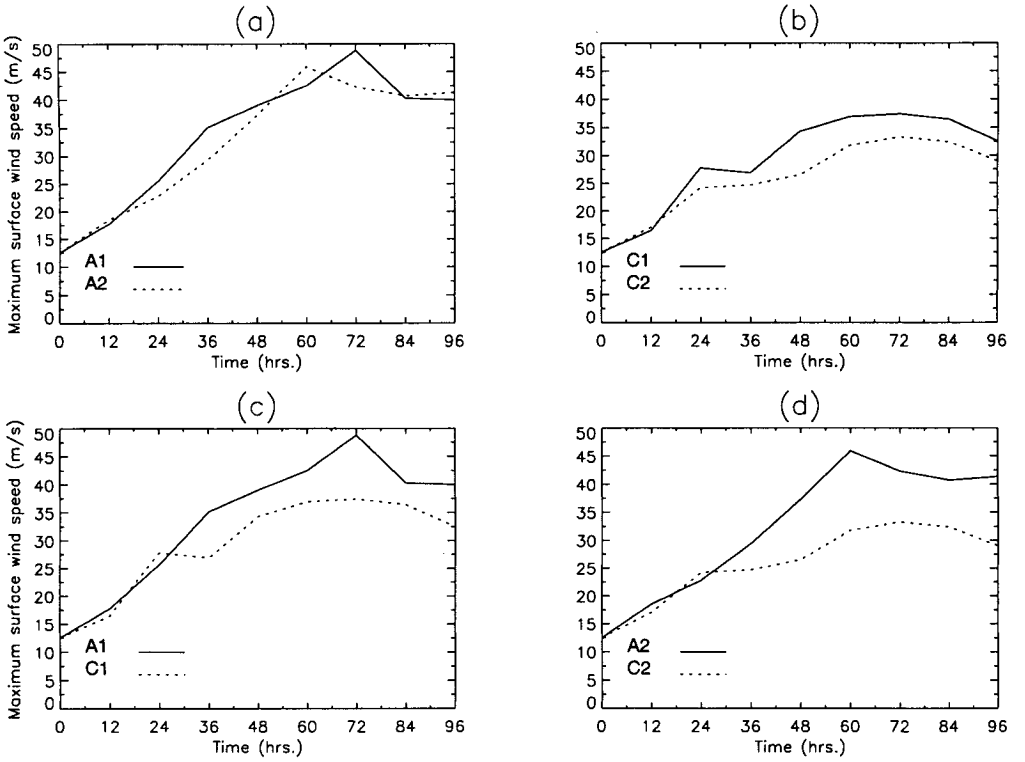

FIG. 9. Comparison of the maximum surface wind speed between (a) experiments A1 and A2; (b) C1 and C2; (c) A1 and C1; (d) A2 and C2.

imum surface pressure and 4.5 m s^{-1} in maximum surface wind. Between A2 and C2 it is 5.4 hPa and 6.6 m s^{-1}, respectively. In similar experiments, Bender et al. (1993) obtained differences of 9.7 hPa and 3.7 m s^{-1}, respectively, and Khain and Ginis (1991) obtained a minimum surface pressure difference of 6.6 hPa. All of these simulations indicate that a small, but significant, reduction in intensity occurs due to surface cooling associated with storm-induced turbulent mixing and upwelling. The differences in the magnitudes from one simulation to another are due to cyclone size, experimental design, and resolution. For example, Bender et al. use a model with finer horizontal resolution and coarser vertical resolution than ours.

Figures 8b and 9b and the last two columns in Table 1 compare the results of the coupled model experiments with bathymetry and land–sea differences (C2) with those without these influences (C1). The differences in minimum surface pressure and maximum surface wind speeds of 3.1 hPa and 4.1 m s^{-1}, respectively, are smaller than those due to coupling, but larger than those due to land–sea differences alone (Figs. 8a, 9a, and columns 2 and 3 in Table 1). The latter observation suggests that, in addition to land–sea contrasts, bathymetry also contributes to the reduction of hurricane intensity. Inspection of Figs. 10–13 suggests why this is so. Figures 10 and 11 show, respectively, the ocean currents at a depth of 500 m in the absence and in the presence of land–sea contrasts and bathymetry. The latter figure reveals strong coastal ocean currents due to the bathymetry. These inertially forced currents enhance the turbulent mixing and upwelling of colder water near the coast. As can be seen in Fig. 12 (which gives the SST difference at two different times between C1 and C2) the enhanced cooling near the coast is of greater magnitude and covers a larger area than the reduced cooling in the deeper water. The time variation of the minimum ocean temperature in the two experiments, shown in Fig. 13, depicts the more dramatic reduction of the SST in the coastal regions when bathymetry is incorporated in the model. Although the center of lowest surface pressure in the storm is far from the coast, hurricane development is influenced by the coastal water temperatures because of the large-scale structure of the disturbance. The extent of this influence is revealed in Figs. 8b and 9b and in Table 1.

Finally, as found by Cooper and Thompson in an uncoupled ocean model, Fig. 14 shows the presence of a storm surge along the coasts associated with the hurricane forcing.

6. Conclusions and suggestions for future research

Based on numerical simulations of a developing tropical storm in the Gulf of Mexico with an uncoupled atmospheric model and a coupled ocean–atmosphere

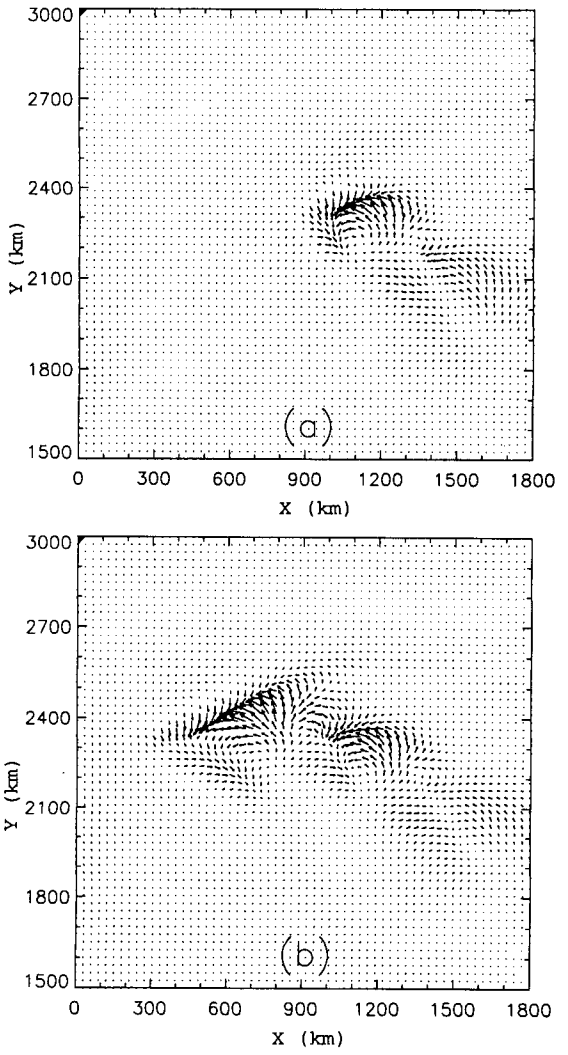

FIG. 10. Deep ocean currents in the absence of land–sea contrasts (C1) at (a) day 3 and (b) day 4. The values are at a depth of 500 m.

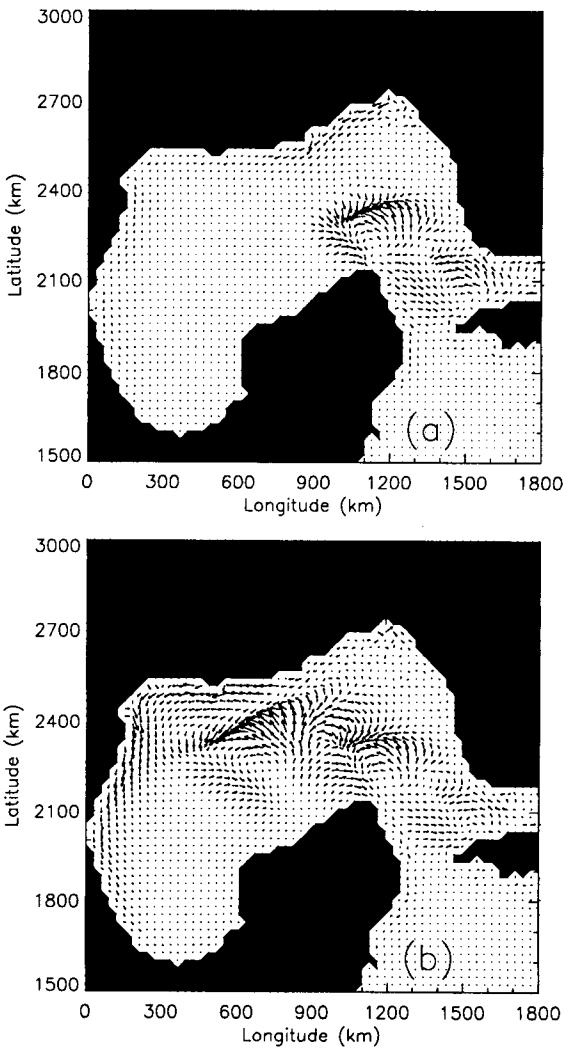

FIG. 11. Deep ocean currents with the land–sea contrasts (C2) at (a) day 3 and (b) day 4. The values are at a depth of 500 m.

model, with and without land–sea contrasts and bathymetry, our primary conclusions, which must be considered to be preliminary in nature for reasons to be discussed below, are that land–sea contrasts and bathymetry both play a role in reducing the intensity of the storm, even when it is far from the coast. Owing to the characteristically large areal extent of tropical storms, drier air coming off the landmasses surrounding the Gulf of Mexico (which can penetrate to the storm center in a day) reduces the moisture supply, and therefore the rate of intensification of the disturbance, when land–sea contrasts are included. Bathymetry acts to cool the sea surface by intensifying the deep water currents, turbulent mixing, and upwelling near the coast. This excess cooling in coastal regions is greater in magnitude and area covered than the reduced cooling that occurs in the deep water and is responsible for a small but significant reduction in the intensity of the storm.

Our conclusions are based on the use of a crude parameterization of land processes, assuming only that the drag coefficient for momentum is much greater and that for heat and moisture exchanges is much smaller than over the ocean. A suggested future study would be one in which radiation processes are taken into account to predict the land temperature as a function of cloudiness and time of day as done by Tuleya (1994) in studying the effect of the land as a hurricane impinges on it. Another future study would be of the ocean response to an atmospheric disturbance in a realistic ocean basin with open boundaries and preexisting ocean currents characteristic of the region.

The atmospheric model we have employed uses the Kuo (1974) parameterization for cumulus convection. This parameterization relies on moisture convergence

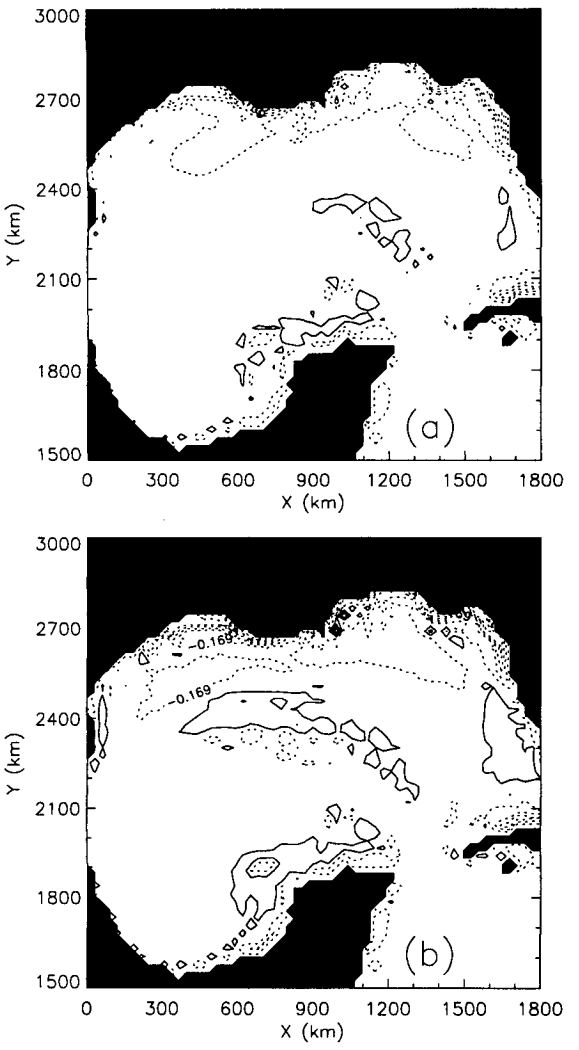

FIG. 12. Difference in SST cooling (C2 − C1) at (a) day 3 and (b) day 4. Contour interval is 0.3°C. The solid lines are positive showing the places where C1 has more surface cooling whereas the dashed lines are negative showing where C2 has more cooling.

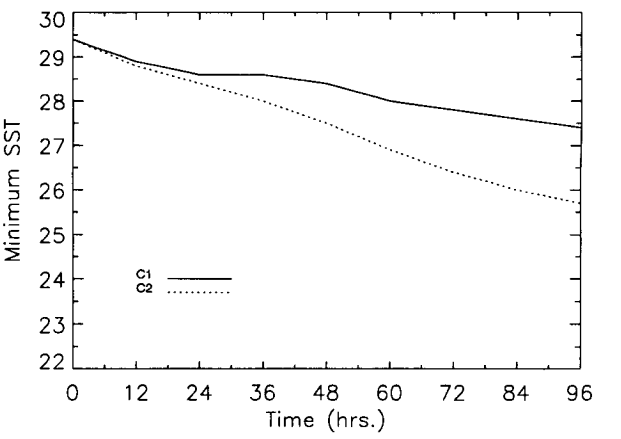

FIG. 13. Time variation of minimum SST for C1 and C2. The units are in °C.

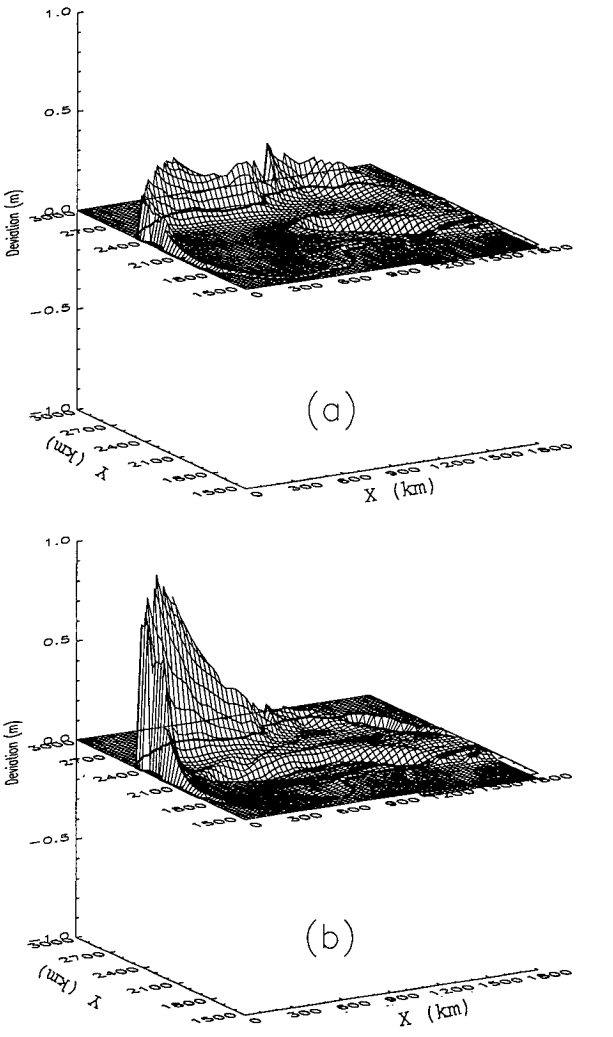

FIG. 14. Surface pressure of the ocean converted to height with the land–sea contrasts and bathymetry (C2) at (a) day 3 and (b) day 4. The values are at a depth of 5 m.

and lifting to set off convection and the release of latent heat that fuels the intensification of the storm. Before definitive conclusions can be reached about the effect of drier air coming off the land on a storm some distance from the the coast, an investigation should be made with one or more different convective parameterizations (e.g., Arakawa and Schubert 1974; Emanuel 1991) that rely on convective instability rather than moisture convergence and lifting to set off cumulus convection.

Acknowledgments. This study was conducted at the Supercomputer Computations Research Institute (SCRI) and Geophysical Fluid Dynamics Institute (GFDI) at The Florida State University, with support from NSF Grant ATM-9310119. The lead author benefited from helpful discussions with Drs. Malakondayya Challa and Ruby Krishnamurti of GFDI.

REFERENCES

Arakawa, A., and W. H. Schubert, 1974: Interaction of a cumulus cloud ensemble with the large-scale environment, Part I. *J. Atmos. Sci.*, **31,** 674–701.

Bender, M. A., I. Ginis, and Y. Kurihara, 1993: Numerical simulations of tropical cyclone ocean interaction with a high-resolution coupled model. *J. Geophys. Res.*, **98,** 23 245–23 263.

Bottomley, M., C. K. Folland, J. Hsiung, R. E. Newell, and D. E. Parker, 1990: *Global Ocean Surface Temperature Atlas.* U. K. Meteorological Office and Massachusetts Institute of Technology, 207 pp.

Challa, M., and R. L. Pfeffer, 1990: Formulation of Atlantic hurricanes from cloud clusters and depressions. *J. Atmos. Sci.*, **47,** 909–927.

——, ——, Q. Zhao, and S. W. Chang 1998: Can eddy fluxes serve as a catalyst for hurricane and typhoon formation? *J. Atmos. Sci.*, **55,** 2201–2219.

Chang, S. W., 1985: Deep ocean response to hurricane as revealed by an ocean model with free surface. Part I: Axisymmetric case. *J. Phys. Oceanogr.*, **15,** 1847–1858.

——, and R. A. Anthes, 1978: Numerical simulations of the ocean's nonlinear, baroclinic response to translating hurricanes. *J. Phys. Oceanogr.*, **8,** 468–480.

——, and ——, 1979: The mutual response of the tropical cyclone and the ocean. *J. Phys. Oceanogr.*, **9,** 128–135.

——, and R. V. Madala, 1980: Numerical simulation of the influence of sea surface temperature on translating tropical cyclones. *J. Atmos. Sci.*, **37,** 2617–2630.

Cooper, C., and J. D. Thompson, 1989: Hurricane-generated currents on the outer continental shelf. Part II: Model sensitivity studies. *J. Geophys. Res.*, **94,** 12 540–12 554.

Cubukcu, N., 1997: A study of the ocean influences on a hurricane using a coupled ocean model with bathymetry and land-sea contrast. M.S. thesis, Dept. of Meteorology, The Florida State University, 121 pp. [Available from Dept. of Meteorology, Love Bldg., The Florida State University, Tallahassee, FL 32306.]

Dietrich, D. E., 1993: Sandia ocean modeling system programmer's guide and user's manual. Sandia National Laboratories, Contract 55-5880, 52 pp. [Available from Sandia National Laboratories, Albuquerque, NM 87185.]

——, and P. J. Roache, 1991: An accurate low dissipation model of the Gulf of Mexico circulation. *Proc. Int. Symp. on Environmental Hydraulics,* Hong Kong, China, 901–909.

——, and D.-S. Ko, 1994: A semi-collocated ocean model based on the SOMS approach. *Int. J. Numer. Methods Fluids,* **19,** 1103–1113.

——, and C. A. Lin, 1994: Numerical studies of eddy shedding in the Gulf of Mexico. *J. Geophys. Res.*, **99,** 7599–7615.

——, M. G. Marietta, and P. J. Roache, 1987: An ocean modeling system with turbulent boundary layers and topography: Numerical description. *Int. J. Numer. Methods Fluids,* **7,** 833–855.

Emanuel, K. A, 1991: A scheme for representing cumulus convection in large-scale models. *J. Atmos. Sci.*, **48,** 2313–2335.

Ginis, I., and Kh. Zh. Dikinov, 1989: Modeling of the Typhoon Virginia (1978) forcing on the ocean. *Sov. Meteor. Hydrol. Rev. Engl. Transl.*, **7,** 53–60.

Khain, A. P., and I. Ginis, 1991: The mutual response of a moving tropical cyclone and the ocean. *Beitr. Phys. Atmos.*, **64,** 125–141.

Kuo, H. L., 1974: Further studies of the parameterization of the influence of cumulus convection in large-scale flow. *J. Atmos. Sci.*, **31,** 1232–1240.

Kurihara, Y., and R. E. Tuleya, 1974: Structure of a tropical cyclone in a three-dimensional numerical simulation model. *J. Atmos. Sci.*, **31,** 893–919.

Leipper, D. L., 1967: Observed ocean conditions and hurricane Hilda, 1964. *J. Atmos. Sci.*, **24,** 182–196.

Levitus, S., 1982: *Climatological Atlas of the World Ocean.* NOAA Prof. Paper 13, 173 pp.

Madala, R. V., S. W. Chang, U. C. Mohanty, S. C. Madan, R. K. Paliwal, V. B. Sarin, T. Holt, and S. Raman, 1987: Description of Naval Research Laboratory limited area dynamical weather prediction model. NRL Tech. Rep. 5992, Washington, DC, 131 pp. [Available from Naval Research Laboratory, Washington, DC 20375-5000.]

Mao, Q., 1994: Numerical simulation of tropical cyclones in a coupled atmosphere–ocean model with nonuniform mixed layer depth. Ph.D. dissertation, The Florida State University, 180 pp. [Available from Dept. of Meteorology, Love Bldg., The Florida State University, Tallahassee, FL 32306.]

McBride, J., and R. Zehr, 1981: Observational analysis of tropical cyclone formation. Part I: Basic description of data sets. *J. Atmos. Sci.*, **38,** 1117–1131.

O'Brien, J. J., and R. O. Reid, 1967: The non-linear response of a two-layer baroclinic ocean to a stationary, axially-symmetric hurricane. Part I: Upwelling induced by momentum transfer. *J. Atmos. Sci.*, **24,** 197–207.

Pfeffer, R. L., and M. Challa, 1981: A numerical study of the role of eddy fluxes of momentum in the development of Atlantic hurricanes. *J. Atmos. Sci.*, **38,** 2393–2398.

——, and ——, 1992: The role of environmental asymmetries in Atlantic hurricane formation. *J. Atmos. Sci.*, **49,** 1051–1059.

——, ——, N. LaSeur, and W. Gray, 1990: Composite Atlantic tropical disturbance structure: Developing and non-developing disturbances. Florida State University Publication, 96 pp. [Available from Geophysical Dynamics Institute, Keen Bldg., The Florida State University, Tallahassee, FL 32306.]

Price, J. F., 1981: Upper ocean response to a hurricane. *J. Phys. Oceanogr.*, **11,** 153–175.

Roache, P. J., and D. E. Dietrich, 1988: Evaluation of the filtered leapfrog-trapezoidal time integration method. *Numer. Heat Transfer,* **14,** 149–164.

Rosenthal, S. L., 1978: Numerical simulation of tropical cyclone development with latent heat by resolvable scales. Part I: Model description and preliminary results. *J. Atmos. Sci.*, **35,** 258–271.

Sanford, T. B., P. G. Black, J. R. Haustein, J. W. Feeney, G. Z. Forristall, and J. F. Price, 1987: Ocean response to a hurricane. Part I: Observations. *J. Phys. Oceanogr.*, **17,** 2065–2083.

Sundqvist, H., 1970: Numerical simulation of the development of tropical cyclones with a ten level model. Part 1. *Tellus,* **22,** 359–390.

Sutyrin, G. G., and A. P. Khain, 1979: Interaction of the ocean and the atmosphere in the area of moving tropical cyclone. *Dokl. Akad. Sci. USSR,* **249,** 467–470.

——, and ——, 1984: On the effect of air–ocean interaction on intensity of moving tropical cyclone. *Atmos. Oceanic Phys.*, **20,** 697–703.

Tuleya, R. E., 1994: Tropical storm development and decay: Sensitivity to surface boundary conditions. *Mon. Wea. Rev.*, **122,** 291–304.

——, M. A. Bender, and Y. Kurihara, 1984: A simulation of the landfall of tropical cyclones using a movable nested-mesh model. *Mon. Wea. Rev.*, **112,** 124–136.